

H₂ fluorescent emission from the diffuse interstellar medium

DAVID A. NEUFELD¹

¹*William H. Miller Department of Physics & Astronomy, Johns Hopkins University, Baltimore, MD 21218, USA*

ABSTRACT

A simple analytic model is presented to predict the near-IR H₂ fluorescent line intensities emitted by diffuse interstellar clouds with a Plummer density profile. It is applicable to sightlines where (1) the column densities of H and H₂ have been measured and (2) the peak gas density can be estimated from extinction maps or observations of C₂ absorption.

1. INTRODUCTION

Several recent developments motivate renewed interest in the H₂ fluorescent emissions expected from the diffuse interstellar medium. Three-dimensional extinction maps (Edenhofer et al. 2024, and references therein) based on recent *Gaia* observations provide unique information about the density structure of the interstellar medium. They suggest that cold diffuse clouds, rather than being at constant density, show a centrally-peaked density profile that is well fit (Zucker et al. 2021; hereafter Z21) by a double Gaussian or by a Plummer profile of the form $n_{\text{H}}(r) = n_0(1 + r^2/r_0^2)^{-p/2}$, where $n_{\text{H}} = n(\text{H}) + 2n(\text{H}_2)$ is the density of H nuclei, n_0 is the density at the cloud center, r is the distance from the cloud center, and r_0 is a constant. In a sample of nearby molecular clouds, Z21 obtained a median power-law index, p , of 1.8 (with a range of 1.2 – 3.4) and a median peak density, n_c , of 49 cm⁻³ (with a range of 35 to 117 cm⁻³). For a ray passing through such a cloud with impact parameter, b , the one-dimensional density profile along the sightline also has a Plummer profile:

$$n_{\text{H}}(z) = \frac{n_{\text{max}}}{(1 + z^2/z_0^2)^{p/2}}, \quad (1)$$

with $z_0 = (r_0^2 + b^2)^{1/2}$ and $n_{\text{max}} = n_0(1 + b^2/r_0^2)^{-p/2}$. Here n_{max} is the peak density along the sightline and z is the distance along the sightline from the location where that peak occurs.

Along the sightlines to hot stars, ultraviolet absorption-line observations can be used to measure the column densities of atomic and molecular hydrogen, $N(\text{H})$ and $N(\text{H}_2)$, providing valuable ancillary information about the molecular fraction (e.g. Obolentseva et al. 2024, and references therein). Moreover, optical and UV observations of individual C₂ rotational states – interpreted using newly-available molecular

data (Najar & Kalugina 2020) – can provide an independent estimate of the peak density of H nuclei, n_{\max} , along such sightlines; for nearby clouds, where the extinction maps are most reliable, such C_2 -derived density estimates are in good agreement with those offered by the extinction maps (Neufeld et al. 2024).

Near-IR spectroscopy, which can now be performed at unprecedented sensitivity with the NIRSpec instrument on JWST, will offer another potential probe of diffuse clouds through the observation of H_2 fluorescent emissions. Whereas previous observations of interstellar H_2 fluorescent emissions were primarily confined to dense clouds lying close to a source of UV radiation (e.g. Le et al 2017), JWST opens the possibility of detecting such emissions from diffuse molecular clouds exposed to the average radiation field in the Galaxy.

In this research note, I present a simple analytic model that may be used to obtain an estimate of the fluorescent H_2 emissions along sightlines of known $N(H)$, $N(H_2)$, and n_{\max} .

2. CALCULATION

For cold gas at densities below $\sim 10^3 \text{ cm}^{-3}$, the intensity of H_2 fluorescent emission is a measure of the photodissociation rate, both processes being caused by the absorption of ultraviolet photons in the Lyman and Werner bands of H_2 . For gas in chemical equilibrium, with the H_2 destruction rate dominated by photodissociation and balanced by the formation rate via grain catalysis, the fluorescent intensity, in any given H_2 line is given by

$$I_f = \frac{(1 - f_a)}{4\pi} \int R n_H n(H) E dz, \quad (2)$$

(Neufeld & Spaans 1996, hereafter NS96) where z is the distance along the line-of-sight, R is the rate coefficient for H_2 formation on grains, E is the mean energy per dissociation emitted in the line under consideration, and f_a is the fraction of the emitted radiation that is absorbed by dust before it reaches us. If we approximate R and E as constant along the sightline (NS96), we obtain $I_f = (1 - f_a) R N(H) \bar{n} E / (4\pi)$, where \bar{n} is the $n(H)$ -weighted average of n_H ,

$$\bar{n} = \frac{1}{N(H)} \int n_H n(H) dz. \quad (3)$$

For a uniform cloud of constant density, \bar{n} is trivially equal to the peak density, n_{\max} , but for a centrally-peaked density distribution \bar{n} is invariably less than n_{\max} . For a Plummer density profile, the solution is relatively simple for the specific case where $p = 2$. The total column density of H nuclei, N_H , is given by

$$N_H = \int \frac{n_{\max} dz}{1 + z^2/z_0^2} = \pi n_{\max} z_0. \quad (4)$$

Because of the increasing density and shielding H_2 column, the molecular fraction increases rapidly as $|z|$ decreases. This motivates a Stromgren-like approximation

(SLA), in which the gas is assumed to be fully molecular for $|z| < z_s$ and fully atomic for $|z| > z_s$. With this approximation, the H_2 column density is

$$N(\text{H}_2) = \frac{1}{2} \int_{-z_s}^{+z_s} \frac{n_{\max} dz}{(1 + z^2/z_0^2)} = n_{\max} z_0 \tan^{-1}(z_s/z_0). \quad (5)$$

Thus z_s is related to the average molecular fraction along the sightline, $f_{\text{H}_2} = 2N(\text{H}_2)/N_{\text{H}}$, by the expression

$$f_{\text{H}_2} = \frac{2 \tan^{-1}(z_s/z_0)}{\pi}, \quad (6)$$

or equivalently $z_s = z_0 \tan(\pi f_{\text{H}_2}/2)$. We may now obtain \bar{n} in the form

$$\bar{n} = \frac{1}{N(\text{H})} \int n_{\text{H}}^2 x(\text{H}) dz = \frac{n_{\max}}{N(\text{H})} \int \frac{x(\text{H}) n_{\max} dz}{(1 + z^2/z_0^2)^2} \quad (7)$$

where $x(\text{H}) = n(\text{H})/n_{\text{H}}$. With the SLA, we obtain

$$\frac{\bar{n}}{n_{\max}} = \frac{2}{N(\text{H})} \int_y^{\infty} \frac{n_{\max} dz}{(1 + z^2/z_0^2)^2} = \left[\frac{\pi}{2} - \frac{y}{1 + y^2} - \tan^{-1} y \right] n_{\max} z_0, \quad (8)$$

where $y = z_s/z_0 = \tan(\pi f_{\text{H}_2}/2)$. Substituting for this expression for y into equation (8), and making use of well-known trigonometric identities, we finally obtain

$$\frac{\bar{n}}{n_{\max}} = \frac{1}{2} - \left(\frac{\sin(\pi f_{\text{H}_2})}{2\pi(1 - f_{\text{H}_2})} \right) = \frac{1 - \text{sinc}(\pi[1 - f_{\text{H}_2}])}{2} \quad (9)$$

For Plummer indices, p , other than 2, the computation of \bar{n} is more complicated, but analytic solutions to the relevant integrals can still be found in terms of the Gaussian (a.k.a. ordinary) hypergeometric function ${}_2F_1(a, b; c; d)$ (SciPy special function `scipy.special.hyp2f1`). The generalizations of equations (6) and (8) are

$$f_{\text{H}_2} = \frac{2}{\sqrt{\pi}} \left(\frac{{}_2F_1(\frac{1}{2}, \frac{p}{2}; \frac{3}{2}; -y^2) y \Gamma(\frac{p}{2})}{\Gamma(\frac{p}{2} - \frac{1}{2})} \right), \quad (10)$$

and

$$\frac{\bar{n}}{n_{\max}} = \frac{{}_2F_1(\frac{1}{2}, p; \frac{3}{2}; -y^2) y - \frac{1}{2} \Gamma(p - \frac{1}{2}) \pi^{1/2} / \Gamma(p)}{{}_2F_1(\frac{1}{2}, \frac{p}{2}; \frac{3}{2}; -y^2) y - \frac{1}{2} \Gamma(\frac{p}{2} - \frac{1}{2}) \pi^{1/2} / \Gamma(\frac{p}{2})}. \quad (11)$$

3. RESULTS

Figure 1 (upper panel) shows the quantity \bar{n}/n_{\max} (eqn. 11) as a function of the sightline-averaged molecular fraction, f_{H_2} (eqn. 10). Results are shown for power-law indices of 1.6, 2.0, 2.4, 2.8, and 3.2 (magenta, cyan, blue, green, and red curves respectively). The results given for $p = 2$ by equation (9) are overplotted with the black dashed curve as a check. The value of \bar{n}/n_{\max} is a decreasing function of f_{H_2} , a behavior that reflects the fact that the atomic region moves outward to gas of lower density as the molecular fraction increases. The use of the SLA to obtain these

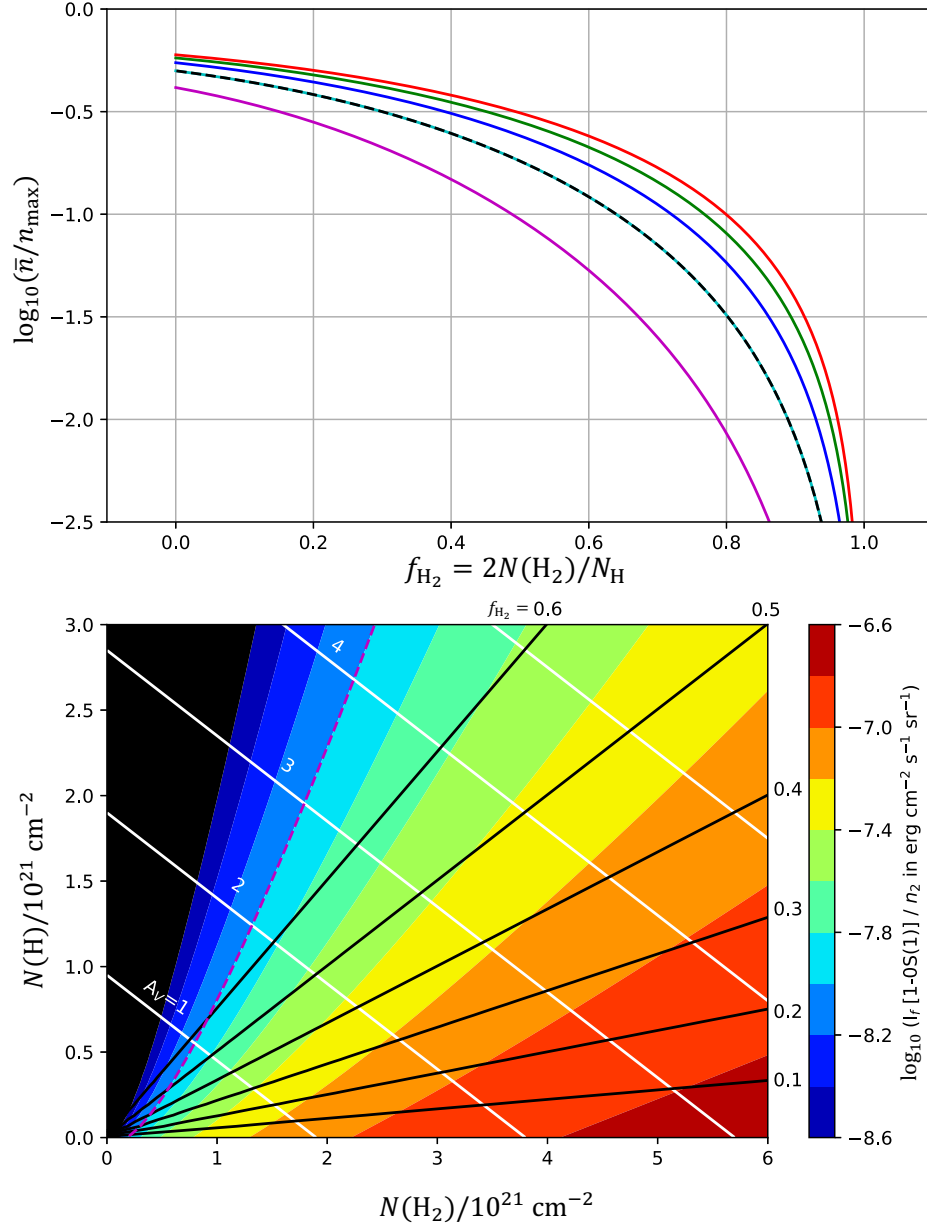


Figure 1. Results of the analytic treatment presented here (see the text for details). Upper panel: \bar{n}/n_{\max} versus f_{H_2} , for Plummer density profiles with power-law indices, p , of 1.6, 2.0, 2.4, 2.8, and 3.2 (magenta, cyan, blue, green, and red curves respectively). Lower panel: predicted fluorescent line intensities for the $v = 1 - 0S(1)$ transition at $2.122 \mu\text{m}$, divided by n_2 .

results means that they may be regarded as lower limits on the actual \bar{n}/n_{\max} : if $x(\text{H})$ exceeds zero for $|z| < z_s$, then more of the atomic hydrogen column is located at higher densities than was assumed.

The lower panel of Figure 1 shows predictions for

$$\frac{I_f}{n_2} = 10^2 \text{ cm}^{-3} (1 - f_a) \frac{RN(\text{H}) E}{4\pi} \left(\frac{\bar{n}}{n_{\max}} \right), \quad (12)$$

where $n_2 = n_{\max}/[10^2 \text{ cm}^{-3}]$. They apply to the $v=1-0 \text{ S}(1)$ transition, and are shown in the plane of the two key observables $N(\text{H})$ and $N(\text{H}_2)$. To obtain the results shown in this plot, I adopted the expression for $(1 - f_a)$ given by NS96; a value for R of $3 \times 10^{-17} \text{ cm}^3 \text{ s}^{-1}$; and a value for E of $4.6 \times 10^{-13} \text{ erg}$, the latter having been computed by NS96 for a typical H_2 ortho-to-para ratio of unity. Parallel white lines show the loci of constant line-of-sight extinction, A_V , for an assumed N_{H}/A_V ratio of $1.9 \times 10^{21} \text{ cm}^{-2}$ per mag, with the A_V values denoted by white numerals. Loci of constant f_{H_2} are also shown in black with their f_{H_2} values labeled with red numerals. For $n_2 = 1$, the dashed magenta line shows the typical JWST/NIRSpec detection limit with the multishutter array (Padovani et al. 2022) of $10^{-8} \text{ erg cm}^{-2} \text{ s}^{-1} \text{ sr}^{-1}$ (3σ in 1.25 hr using 25 shutters).

The results presented here apply specifically to gas in chemical equilibrium. As noted by Goldshmidt & Sternberg (1995) and by Bialy et al. (2024), if the H_2 abundance is out of equilibrium and increasing (decreasing) with a destruction rate smaller (larger) than the formation rate, then the expected line intensity will be smaller (larger) than the values plotted in the lower panel of Figure 1.

I am pleased to acknowledge helpful discussions with S. Bialy.

REFERENCES

- Bialy, S., Burkhart, B., Seifried, D., et al. 2024, arXiv:2408.06416.
doi:10.48550/arXiv.2408.06416
- Edenhofer, G., Zucker, C., Frank, P., et al. 2024, *A&A*, 685, A82.
doi:10.1051/0004-6361/202347628
- Goldshmidt, O. & Sternberg, A. 1995, *ApJ*, 439, 256. doi:10.1086/175168
- Le, H. A. N., Pak, S., Kaplan, K., et al. 2017, *ApJ*, 841, 13.
doi:10.3847/1538-4357/aa6bf7
- Najar, F. & Kalugina, Y. 2020, *RSC Advances*, 10, 8580.
doi:10.1039/C9RA10319H
- Neufeld, D. A. & Spaans, M. 1996, *ApJ*, 473, 894. doi:10.1086/178201
- Neufeld, D. A., Welty, D. E., Ivlev, A. V., et al. 2024, arXiv:2408.11108.
doi:10.48550/arXiv.2408.11108
- Obolentseva, M., Ivlev, A. V., Silsbee, K., et al. 2024, arXiv:2408.11511.
doi:10.48550/arXiv.2408.11511
- Padovani, M., Bialy, S., Galli, D., et al. 2022, *A&A*, 658, A189.
doi:10.1051/0004-6361/202142560
- Zucker, C., Goodman, A., Alves, J., et al. 2021, *ApJ*, 919, 35.
doi:10.3847/1538-4357/ac1f96